Physics Letters B 674 (2009) 103–110

Contents lists available at ScienceDirect

Physics Letters B

www.elsevier.com/locate/physletb

Nonmesonic weak decay spectra of ${}^{4}_{\Lambda}$He

E. Bauer [a,e], A.P. Galeão [b], M.S. Hussein [c,f], F. Krmpotić [c,e,g,*], J.D. Parker [d]

[a] Facultad de Ciencias Exactas, Departamento de Física, Universidad Nacional de La Plata, 1900 La Plata, Argentina
[b] Instituto de Física Teórica, Universidade Estadual Paulista, Rua Pamplona 145, 01405-900 São Paulo, SP, Brazil
[c] Departamento de Física Matemática, Instituto de Física da Universidade de São Paulo, Caixa Postal 66318, 05315-970 São Paulo, SP, Brazil
[d] Department of Physics, Kyoto University, Kyoto 606-8502, Japan
[e] Instituto de Física La Plata, CONICET, 1900 La Plata, Argentina
[f] Max-Planck-Institut für Physik komplexer Systeme, Nöthnitzer Straße, 38, D-01187 Dresden, Germany
[g] Facultad de Ciencias Astronómicas y Geofísicas, Universidad Nacional de La Plata, 1900 La Plata, Argentina

ARTICLE INFO

Article history:
Received 14 June 2008
Received in revised form 2 December 2008
Accepted 27 January 2009
Available online 10 March 2009
Editor: J.-P. Blaizot

PACS:
21.80.+a
13.75.Ev
27.10.+h

Keywords:
Nonmesonic decay
One-nucleon spectra
Two-nucleon spectra
One-meson-exchange model
s-Shell hypernuclei
Independent-particle shell model

ABSTRACT

To comprehend the recent Brookhaven National Laboratory experiment E788 on ${}^{4}_{\Lambda}$He, we have outlined a simple theoretical framework, based on the independent-particle shell model, for the one-nucleon-induced nonmesonic weak decay spectra. Basically, the shapes of all the spectra are tailored by the kinematics of the corresponding phase space, depending very weakly on the dynamics, which is gauged here by the one-meson-exchange potential. In spite of the straightforwardness of the approach a good agreement with data is achieved. This might be an indication that the final-state-interactions and the two-nucleon induced processes are not very important in the decay of this hypernucleus. We have also found that the $\pi + K$ exchange potential with soft vertex-form-factor cutoffs ($\Lambda_\pi \approx 0.7$ GeV, $\Lambda_K \approx 0.9$ GeV), is able to account simultaneously for the available experimental data related to Γ_p and Γ_n for ${}^{4}_{\Lambda}$H, ${}^{4}_{\Lambda}$He, and ${}^{5}_{\Lambda}$He.

The nonmesonic weak decay (NMWD) of Λ hypernuclei, $\Lambda N \to nN$ ($N = p, n$), is very interesting in several aspects. First, it implies the most radical mutation of an elementary particle when embedded in a nuclear environment: without producing any additional on-shell particle, as does the mesonic weak decay $\Lambda \to \pi N$, the mass is changed by 176 MeV, and the strangeness by $\Delta S = 1$. Second, it is the main decay channel for medium and heavy hypernuclei. Third, as such it offers the best opportunity to examine the strangeness-changing nonleptonic weak interaction between hadrons. Fourth, it plays a dominant role in the stability of rotating neutron stars with respect to gravitational wave emission [1,2]. Finally, with the incorporation of strangeness, the (N, Z) radioactivity domain is extended to three dimensions (N, Z, S). Therefore, the understanding of the NMWD cannot but help to advance our knowledge of physics.

Several important experimental advances in NMWD have been made in recent years, which have allowed to establish more precise values of the neutron- and proton-induced transition rates $\Gamma_n \equiv \Gamma(\Lambda n \to nn)$ and $\Gamma_p \equiv \Gamma(\Lambda p \to np)$, solving in this way the long-standing puzzle of the branching ratio $\Gamma_{n/p} \equiv \Gamma_n/\Gamma_p$. They are: (1) the new high quality measurements of single-nucleon spectra $S_N(E)$, as a function of one-nucleon energy $E_N \equiv E$ done in Refs. [3–6], and (2) the first measurements of the two-particle-coincidence spectra as a function of the sum of kinetic energies $E_n + E_N \equiv E$, $S_{nN}(E)$, and of the opening angle $\theta_{nN} \equiv \theta$, $S_{nN}(\cos\theta)$, done in Refs. [6–11].

Particularly interesting is the Brookhaven National Laboratory experiment E788 on ${}^{4}_{\Lambda}$He, performed by Parker et al. [6], which highlighted that the effects of the Final State Interactions (FSI) on the one-nucleon induced decay, as well as the contributions of the two-nucleon induced decays, $\Lambda NN \to nNN$, could be very small in this case, if any. Therefore one might hope that the Independent Particle Shell Model (IPSM) [12–17] could be an adequate framework to account for the NMWD spectra of this hypernucleus. The aim of the present work is to verify this expectation.

* Corresponding author at: Departamento de Física Matemática, Instituto de Física da Universidade de São Paulo, Caixa Postal 66318, 05315-970 São Paulo, SP, Brazil.
E-mail address: krmpotic@fma.if.usp.br (F. Krmpotić).

0370-2693
doi:10.1016/j.physletb.2009.01.072

To derive the expressions for the NMWD rates we start from the Fermi Golden Rule. For a hypernucleus with spin J_I decaying to residual nuclei with spins J_F, and two free nucleons nN (with total spin S and total kinetic energy $E_{nN} = E_n + E_N$), the transition rate reads [15]

$$\Gamma_N = 2\pi \sum_{SM_S J_F M_F} \int \left|\langle \mathbf{p}_n \mathbf{p}_N S M_S J_F M_F | V | J_I M_I \rangle\right|^2 \times \delta(E_{nN} + E_R - \Delta_N) \frac{d\mathbf{p}_n}{(2\pi)^3} \frac{d\mathbf{p}_N}{(2\pi)^3}. \quad (1)$$

The NMWD dynamics, contained within the weak hypernuclear transition potential V, will be described by the one-meson exchange (OME) model, whose most commonly used version includes the exchange of the full pseudoscalar (π, K, η) and vector (ρ, ω, K^*) meson octets (PSVE), with the weak coupling constants obtained from soft meson theorems and $SU(6)_W$ [12,18]. The wave functions for the kets $|\mathbf{p}_n \mathbf{p}_N S M_S J_F M_F\rangle$ and $|J_I M_I\rangle$ are assumed to be antisymmetrized and normalized, and the two emitted nucleons n and N are described by plane waves. Initial and final short range correlations are included phenomenologically at a simple Jastrow-like level, while the finite nucleon size effects at the interaction vertices are gauged by monopole form factors [12,15]. Moreover,

$$E_R = \frac{|\boldsymbol{p}_n + \boldsymbol{p}_N|^2}{2M(A-2)} = \frac{E_{nN} + 2\cos\theta_{nN}\sqrt{E_n E_N}}{A-2}, \quad (2)$$

is the recoil energy of the residual nucleus, and $\Delta_N \equiv \Delta + e_N + e_\Lambda$ is the liberated energy, with $\Delta = M - M_\Lambda = 176$ MeV, and e_N and e_Λ being the nucleon and hyperon separation energies, which were taken from Refs. [19] and [20] respectively.

Following step by step the developments done in Refs. [21–23], in connection with the asymmetry parameter, Eq. (1) can be cast in the form

$$\Gamma_N = \frac{4}{\pi} \int d\cos\theta \int p_N^2\, dp_N \int p_n^2\, dp_n \times \delta(E_{nN} + E_R - \Delta_N) \mathcal{I}_N(p, P), \quad (3)$$

where the quantity [15,16,22,23]

$$\mathcal{I}_N(p, P) = \sum_{J=0}^{J=1} F_J(N) \sum_{SlT} \mathcal{M}^2(pP, lSJT; N), \quad (4)$$

depends on the spectroscopic factors $F_J(N)$, and on the transition matrix elements $\mathcal{M}(pP, lSJT; N)$. Those, in turn, depend on the c.m. and relative momenta, which are given in terms of the integration variables in (3) by

$$P = \sqrt{(A-2)\big(2M\Delta_N - p_n^2 - p_N^2\big)}, \quad (5)$$

and

$$p = \sqrt{M\Delta_N - \frac{A}{4(A-2)} P^2}, \quad (6)$$

where the energy conservation condition has been used. The correctness of Eq. (3) for $N = p$ can be easily verified by confronting it with the expression [22, Eq. (3.1)] for $\omega_0 \equiv \Gamma_p$, and noticing that the quantity $\sum_{\mathrm{lL}} \mathcal{O}(P; \mathrm{L}) \mathcal{I}_0(p; j_p, \mathrm{l})$ in that reference is equal to $\mathcal{I}_p(p, P)$ here. The relative-space part of the two-body nuclear matrix elements (NME), that govern the NMWD dynamics proper, are contained within the $\mathcal{M}$'s and depend on the momenta only via p (see [22, Eq. (B1)]). Moreover, this p-dependence is very weak in the region of interest and allows to compute the NMEs at the fixed value of $p = \sqrt{M\Delta_N}$ [22,23]. As a consequence this part can be factored out of the integrals in Eq. (3), which explains why only the transition rates, but not the normalized spectra, significantly depend on the intrinsic NMWD dynamics [24]. Notice, however, that the $\mathcal{M}$'s as a whole do strongly depend on P through the center-of-mass overlaps of the two-body wave functions.

Next, the δ-function in (3) can be put in the form

$$\frac{A-2}{A-1} \frac{2M}{|p_n^+ - p_n^-|} \big[\delta(p_n - p_n^+) + \delta(p_n - p_n^-)\big], \quad (7)$$

where

$$p_n^\pm = (A-1)^{-1} \Big[-p_N \cos\theta_{nN} \pm \sqrt{2M(A-2)(A-1)\Delta_N - p_N^2\big[(A-1)^2 - \cos^2\theta_{nN}\big]}\Big]. \quad (8)$$

Doing this, Eq. (3) becomes

$$\Gamma_N = \frac{8M}{\pi} \frac{A-2}{A-1} \int_{-1}^{+1} d\cos\theta_{nN} \int p_N^2\, dp_N \frac{(p_n^+)^2}{|p_n^+ - p_n^-|} \big[\mathcal{I}_N(p, P)\big]_{p_n \to p_n^+} + \big(p_n^+ \leftrightarrow p_n^-\big), \quad (9)$$

where the notation $[\mathcal{I}_N(p, P)]_{p_n \to p_n^+}$ indicates that $\mathcal{I}_N(p, P)$ is to be computed with P and p given by Eqs. (5) and (6) with p_n replaced by p_n^+. We have shown numerically that the last term in (9) is negligibly small in comparison with the first one and therefore it will be omitted from now on. With the simple change of variable $p \to \sqrt{2ME}$ one finally gets

$$\Gamma_N = (A-2) \frac{8M^3}{\pi} \int_{-1}^{+1} d\cos\theta_{nN} \int_0^{E_N^{\max}} dE_N \sqrt{\frac{E_N}{E'_N}} E_n^+ \mathcal{I}_N(p^+, P^+), \quad (10)$$

where

$$E'_N = (A-2)(A-1)\Delta_N - E_N\big[(A-1)^2 - \cos^2\theta_{nN}\big], \quad (11)$$

$$E_n^+ = \Big[\sqrt{E'_N} - \sqrt{E_N}\cos\theta_{nN}\Big]^2 (A-1)^{-2}, \quad (12)$$

and P^+ and p^+ are to be computed from Eqs. (5) and (6) with p_n replaced by p_n^+. It might be worth noticing that, while E'_N does not have a direct physical meaning, E_n^+ is the energy of the neutron that is the decay partner of the nucleon N with energy E_N. The maximum energy of integration in (10) is

$$E_N^{\max} = \frac{A-1}{A} \Delta_N. \quad (13)$$

This ensures that p_n^+, given by Eq. (8), is real. In order to ensure that it also be positive, as it must, one has to enforce the condition

$$\sqrt{E'_N} > \sqrt{E_N}\cos\theta_{nN} \quad (14)$$

throughout the integration.

The decay rate in Eq. (3) can be rewritten in terms of energy variables as

$$\Gamma_N = \frac{8M^3}{\pi} \int d\cos\theta_{nN} \int dE_N \int dE_n \sqrt{E_N E_n} \times \delta(E_{nN} + E_R - \Delta_N) \mathcal{I}_N(p, P), \quad (15)$$

and the energy-conserving δ-function as

$$\frac{A-2}{2\sqrt{E_n E_N}} \delta\big[\cos\theta_{nN} - C_{nN}(E_n, E_N)\big], \quad (16)$$

where

$$C_{nN}(E_n, E_N) = \frac{(A-2)\Delta_N - (A-1)(E_n + E_N)}{2\sqrt{E_n E_N}}. \quad (17)$$

Thus, upon eliminating the delta, one gets

$$\Gamma_N = \frac{4M^3(A-2)}{\pi} \int_0^{E_N^{\max}} dE_N \int_0^{E_N^{\max}} dE_n\, \mathcal{I}_N(p, P), \quad (18)$$

with the constraint

$$-1 < C_{nN}(E_n, E_N) < +1 \tag{19}$$

to be imposed throughout the integration. Here, the variables P and p in $\mathcal{I}_N(p, P)$ can be computed from

$$P = \sqrt{2M(A-2)(\Delta_N - E_n - E_N)} \tag{20}$$

and Eq. (6).

We note that in Ref. [24] the kinetic energy sum spectra have been evaluated from

$$\Gamma_N = \frac{4M^3}{\pi}\sqrt{A(A-2)^3} \times \int_{E_{nN}^{\min}}^{\Delta_N} dE_{nN} \sqrt{(\Delta_N - E_{nN})\big(E_{nN} - E_{nN}^{\min}\big)}\mathcal{I}_N(p, P), \tag{21}$$

with

$$E_{nN}^{\min} = \Delta_N \frac{A-2}{A}, \tag{22}$$

and p and P given by Eq. (6) and

$$P = \sqrt{2M(A-2)(\Delta_N - E_{nN})}. \tag{23}$$

Here, however, in order to be able to take one-nucleon detection energy thresholds into account, it is more convenient to start from Eq. (18) rewritten in the form

$$\Gamma_N = \frac{4M^3(A-2)}{\pi} \int_{E_{nN}^{\min}}^{\Delta_N} dE_{nN} \int_0^{E_N^{\max}} dE_N \times \int_0^{E_N^{\max}} dE_n \mathcal{I}_N(p, P)\delta(E_N + E_n - E_{nN}). \tag{24}$$

To implement angular cuts, one has simply to alter the lower and/or upper limits in inequality (19).

The needed transition probability densities $S_N(E_N)$, $S_{nN}(\cos\theta_{nN})$, and $S_{nN}(E_{nN})$ can now be obtained by performing derivatives on E_N, $\cos\theta_{nN}$, and E_{nN} in the appropriate equation for Γ_N, namely, Eq. (10) or Eq. (18) for the first, Eq. (10) for the second, and Eq. (21) or Eq. (24) for the third one.

The experimental data on NMWD rates in the s-shell are compared in Table 1 with the most recent theoretical results. As can be seen, no calculation, in which the same model and the same parametrization have been employed for all three nuclei, is capable of reproducing all the data, which might imply that no one of them describes the full dynamics of these processes. In particular, using the PSVE model [16] it was not possible to account, either for the ${}^{4}_{\Lambda}$He, or for the ${}^{5}_{\Lambda}$He data, while the potentials constructed by Itonaga et al. [14], from the correlated 2π coupled to ρ and/or σ mesons, are conflicting with the recent ${}^{4}_{\Lambda}$He data for Γ_{nm} and $\Gamma_{n/p}$ [6]. The only calculation done with the PSVE model that reproduces the ${}^{5}_{\Lambda}$He data is the one by Chumillas et al. [31], but, unfortunately, the results for the remaining two s-shell hypernuclei are not given. We have repeated now the calculation done previously in Ref. [16] for the PSVE and the one-$(\pi + K)$ exchange (PKE) models, but with values of the size parameter, b, taken from Ref. [14]: $b({}^{4}_{\Lambda}\mathrm{H}) = b({}^{4}_{\Lambda}\mathrm{He}) = 1.65$ fm, and $b({}^{5}_{\Lambda}\mathrm{He}) = 1.358$ fm. In Table 1, they are labelled, respectively, as P1 and P2, and both are very far from data.[1] We do not know how these b-values have been adjusted, but they seem to be more realistic than those used in Ref. [16]. In fact, they are consistent with the estimate $b = \frac{1}{2}\sqrt{\frac{2}{3}}(R_N + R_\Lambda)$, where R_N and R_Λ are, respectively, the root-mean-square distances of the nucleons and the Λ from the center of mass of the hypernucleus. This yields $b({}^{4}_{\Lambda}\mathrm{H}) = b({}^{4}_{\Lambda}\mathrm{He}) = 1.53$ fm, and $b({}^{5}_{\Lambda}\mathrm{He}) = 1.33$ fm [20]. The relative and the c.m. oscillator parameters are simply evaluated as $b_r = b\sqrt{2}$ and $b_R = b/\sqrt{2}$. We have also tried [26, Eqs. (36) and (37)], used by Inoue et al., but this has little influence on our results.

To improve the agreement we could either: (1) add more mesons, (2) modify the model parameters, or (3) incorporate additional degrees of freedom. We have chosen the second option, trying to use the smallest number of mesons. The simplest possibility is, of course, the one-pion exchange potential. We have found that for the monopole vertex-form-factor cutoff parameter of the pion, $\Lambda_\pi \lesssim 0.7$ GeV, and the size parameter $b \gtrsim 1.6$ fm it is possible to account for the ${}^{4}_{\Lambda}$He data but not for that of ${}^{5}_{\Lambda}$He. Next, we have examined the PKE model, for fixed values of the size parameters b mentioned above. In Fig. 1 is shown the dependence of Γ_N on the π and K cutoff parameters Λ_π and Λ_K. Roughly speaking, $\Gamma_p({}^{4}_{\Lambda}\mathrm{He})$ and $\Gamma_p({}^{5}_{\Lambda}\mathrm{He})$ depend mainly on Λ_π, while $\Gamma_p({}^{4}_{\Lambda}\mathrm{H})$ and $\Gamma_n({}^{4}_{\Lambda}\mathrm{He})$ depend mainly on Λ_K and the other two rates depend with about equal weight on both. The similarities and the differences in the behaviors of Γ_p and Γ_n for the three hypernuclei are mainly due to the spectroscopic factors, exhibited in [16, Table 1]. The b-values also play a significant role. The most relevant issue here is, however, that there is a region of rather soft Λ_π and Λ_K where all the Γ_N are reproduced fairly well.[2] In Table 1 are shown the results for $\Lambda_\pi = 0.7$ GeV and $\Lambda_K = 0.9$ GeV, labelled as P3, which we call the soft $\pi + K$ exchange (SPKE) potential, and which will be used in the evaluation of the NMWD spectra of ${}^{4}_{\Lambda}$He in what follows. We note that they are similar to the results T3, obtained by Sasaki et al. [28] within the PKE model with $\Lambda_\pi = 0.8$ GeV and $\Lambda_K = 1.2$ GeV. It is interesting to remark that the $\Delta T = \frac{1}{2}$ prediction $\frac{\Gamma_n({}^{4}_{\Lambda}\mathrm{He})}{\Gamma_p({}^{4}_{\Lambda}\mathrm{H})} = 2$ is quite well fulfilled for the SPKE model. Yet, the relationship $\frac{\Gamma_n({}^{4}_{\Lambda}\mathrm{H})}{\Gamma_p({}^{4}_{\Lambda}\mathrm{He})} = \frac{\Gamma_n}{\Gamma_p}({}^{5}_{\Lambda}\mathrm{He})$ is satisfied only approximately. The reason for that are the differences in the binding energies and the values of the b parameter.

We are aware that the OME models predict a too large and negative asymmetry parameter a_Λ in ${}^{5}_{\Lambda}$He [13,21–23,28,30], and also that there are two recent proposals to bring this value into agreement with experiments by going beyond the OME model and incorporating new scalar–isoscalar terms. Namely, Chumillas et al. [31] have pointed out that these new terms come from the exchange of correlated 2π coupled to σ, plus uncorrelated 2π exchanges, while Itonaga et al. [32] had to invoke the axial-vector a_1 meson to reproduce the data for a_Λ in ${}^{5}_{\Lambda}$He. The 2π-exchange potentials are rather cumbersome, and it is somewhat controversial to which extent these new mechanisms alter the transition rates. The first group [31] affirms that the 2π exchanges leave them basically unaltered, as seen from the results T7 and T7′ in Table 1. Yet, the second group [32] asserts that the axial-vector

[1] It is more than evident that the value of b is important in scaling the magnitudes of the Γ_N. The differences between the PSVE results shown here and those reported in Ref. [16] arise from the values of b used. In the latter case that value was taken to be $b = \sqrt{\frac{\hbar}{M\omega}}$, with $\hbar\omega = 45A^{-1/3} - 25A^{-2/3}$ MeV. We do not know the origin of the discrepancy with Chumillas et al. [31].

[2] To reproduce the combined effect of short-range correlation and form factor reductions Bennhold and Ramos [33] have used a monopole form factor with a very soft cutoff of $\Lambda_\pi \approx 0.6$ GeV.

Table 1
The NMWD rates in the s-shell. (A) Experimental: E1 [25]: E2 [6]; E3 [8]; E4 [9], (B) Theoretical: T1 – $(\pi + \mathrm{DQ})$ [26]; T2 – $(\pi + 4\mathrm{BPI})$ [27]; T3 – (PKE) [28]; T3′ – $(\pi + K + \mathrm{DQ})$ [28]; T4 – $(\pi + 2\pi/\sigma + 2\pi/\rho + \omega)$ [14]; T5 – (PSVE) [16]; T6 – $(\pi + K + \sigma + \mathrm{DQ})$ [29], T7 – (PSVE) [31]; T7′ – $(\mathrm{PSVE} + 2\pi + 2\pi/\sigma)$ [31]. (C) Present results: P1 – (PSVE); P2 – (PKE); P3 – (SPKE).

	${}^{4}_{\Lambda}$H				${}^{4}_{\Lambda}$He				${}^{5}_{\Lambda}$He			
	Γ_p	Γ_n	Γ_{nm}	$\Gamma_{n/p}$	Γ_p	Γ_n	Γ_{nm}	$\Gamma_{n/p}$	Γ_p	Γ_n	Γ_{nm}	$\Gamma_{n/p}$
(A)												
E1			$0.17^{+0.11}_{-0.11}$		$0.16^{+0.02}_{-0.02}$	$0.01^{+0.04}_{-0.01}$	$0.17^{+0.05}_{-0.05}$	$0.06^{+0.25}_{-0.06}$				
E2					$0.180^{+0.028}_{-0.028}$	$\leqslant 0.035$	$0.177^{+0.029}_{-0.029}$	$\leqslant 0.19$				
E3											$0.424^{+0.024}_{-0.024}$	
E4												$0.45^{+0.14}_{-0.14}$
(B)												
T1	0.047	0.126	0.174	2.66	0.214	0.038	0.253	0.178	0.421	0.206	0.627	0.489
T2	0.034	0.002	0.036	18.2	0.030	0.170	0.200	0.17	0.192	0.174	0.366	1.10
T3	0.005	0.067	0.071	14.2	0.145	0.009	0.155	0.064	0.207	0.097	0.304	0.466
T3′	0.030	0.157	0.187	5.32	0.214	0.004	0.218	0.019	0.304	0.219	0.523	0.720
T4	0.040	0.088	0.128	2.17	0.223	0.081	0.303	0.363	0.305	0.118	0.422	0.386
T5	0.014	0.154	0.168	10.4	0.477	0.030	0.507	0.061	0.461	0.148	0.609	0.320
T6	0.035	0.093	0.128	2.70	0.165	0.069	0.235	0.417	0.253	0.392	0.392	0.548
T7									0.257	0.122	0.474	0.379
T7′									0.275	0.114	0.415	0.388
(C)												
P1	0.014	0.144	0.159	9.98	0.463	0.029	0.492	0.062	0.701	0.229	0.930	0.327
P2	0.005	0.143	0.149	27.9	0.357	0.011	0.368	0.031	0.534	0.231	0.766	0.433
P3	0.005	0.071	0.076	2.70	0.179	0.012	0.191	0.068	0.281	0.121	0.402	0.431

meson contributions, not only bring the asymmetry parameter a_Λ into agreement with recent measurement, but improve also the Γ_n/Γ_p ratio such as to become well comparable to the experimental data. Anyhow, in no one of these works are discussed the transition rates in ${}^{4}_{\Lambda}$He and ${}^{4}_{\Lambda}$H.

The transition probability densities $S_N(E)$, $S_{nN}(E)$, and $S_{nN}(\cos\theta)$ contain the same dynamics, *i.e.*, the same NMEs, but involve different phase-space kinematics for each case. In particular, the proton spectrum $S_p(E)$ is related with the expected number of protons $d\mathrm{N}_p(E)$ detected within the energy interval dE through the relation

$$\frac{d\mathrm{N}_p(E)}{dE} = C_p(E) S_p(E), \tag{25}$$

where $C_p(E)$ depends on the proton experimental environment and includes all quantities and effects not considered in $S_p(E)$, such as the number of produced hypernuclei, the detection efficiency and acceptance, *etc.* In experiment E788, after correction for acceptance, the remaining $C_p(E)$ factor is approximately energy-independent in the region beyond the detection threshold, E_p^0 [34]. In what follows, we will always compare our predictions with the experimental spectra that have been corrected for acceptance and take into account the detection threshold. Thus we can write, for the expected number of detected protons above this threshold,

$$\bar{\mathrm{N}}_p = \int_{E_p^0}^{E_p^{\max}} \frac{d\mathrm{N}_p(E)}{dE} dE = \bar{C}_p \int_{E_p^0}^{E_p^{\max}} S_p(E)\, dE = \bar{C}_p \bar{\Gamma}_p. \tag{26}$$

This allows us to rewrite (25) in the form[3]

$$\frac{d\mathrm{N}_p(E)}{dE} = \bar{\mathrm{N}}_p \frac{S_p(E)}{\bar{\Gamma}_p} \quad \left(E > E_p^0\right). \tag{27}$$

[3] A similar expression is valid for the β-decay strength function (see, for instance, [35, Eq. (5)]).

The spectrum $S_p(E)$ is normalized to the experimental one by replacing $\bar{\mathrm{N}}_p$ in (27) with the acceptance-corrected number of actually observed protons,

$$\bar{\mathrm{N}}_p^{\mathrm{exp}} = \sum_{i=1}^{m} \Delta\mathrm{N}_p^{\mathrm{exp}}(E_i), \tag{28}$$

where $\Delta\mathrm{N}_p^{\mathrm{exp}}(E_i)$ is the acceptance-corrected number of protons measured at energy E_i within a fixed energy bin ΔE_p, and m is the number of bins beyond the detection threshold. Thus, the quantity that we have to confront with data is

$$\Delta\mathrm{N}_p(E) = \bar{\mathrm{N}}_p^{\mathrm{exp}} \Delta E_p \frac{S_p(E)}{\bar{\Gamma}_p}, \tag{29}$$

where the barred symbols ($\bar{\mathrm{N}}_p^{\mathrm{exp}} = 4546$, and $\bar{\Gamma}_p = 0.168$) indicate that the proton threshold $E_p^0 = 40$ MeV [34] has been considered in the numerical evaluation of the corresponding quantities. In contrast to $\Delta\mathrm{N}_p^{\mathrm{exp}}(E_i)$, $\Delta\mathrm{N}_p(E)$ is a continuous function of E.

As the one-proton (one-neutron) induced decay prompts the emission of an np (nn) pair, one has in the same way for the one-neutron spectrum

$$\Delta\mathrm{N}_n(E) = \bar{\mathrm{N}}_n^{\mathrm{exp}} \Delta E_n \frac{S_p(E) + 2S_n(E)}{\bar{\Gamma}_p + 2\bar{\Gamma}_n}. \tag{30}$$

Here, $\bar{\mathrm{N}}_n^{\mathrm{exp}} = 3565$, and $\bar{\Gamma}_p + 2\bar{\Gamma}_n = 0.198$ have been evaluated with a neutron threshold of 30 MeV [34]. In Fig. 2, our results are compared with the measurements of Parker et al. [6].

A similar, but somewhat different, procedure is followed for the coincidence spectra. The main difference arises from the fact that the angular-correlation spectra, $\Delta\mathrm{N}_{nN}^{\mathrm{exp}}(\cos\theta_i)$, as well as the kinetic energy sum data, $\Delta\mathrm{N}_{nN}^{\mathrm{exp}}(E_i)$, besides being acceptance-corrected, were measured with detection thresholds of 30 MeV for both neutrons and protons. More, in the selection of the kinetic energy sum data it was also applied an angular cut of $\cos\theta_{nN} < -0.5$. In order to make the presentation simple, the observables that comprise only the energy cuts, and those that include both the energy and the angular cuts, will be indicated by putting, respectively, a tilde and a hat over the corresponding symbols.

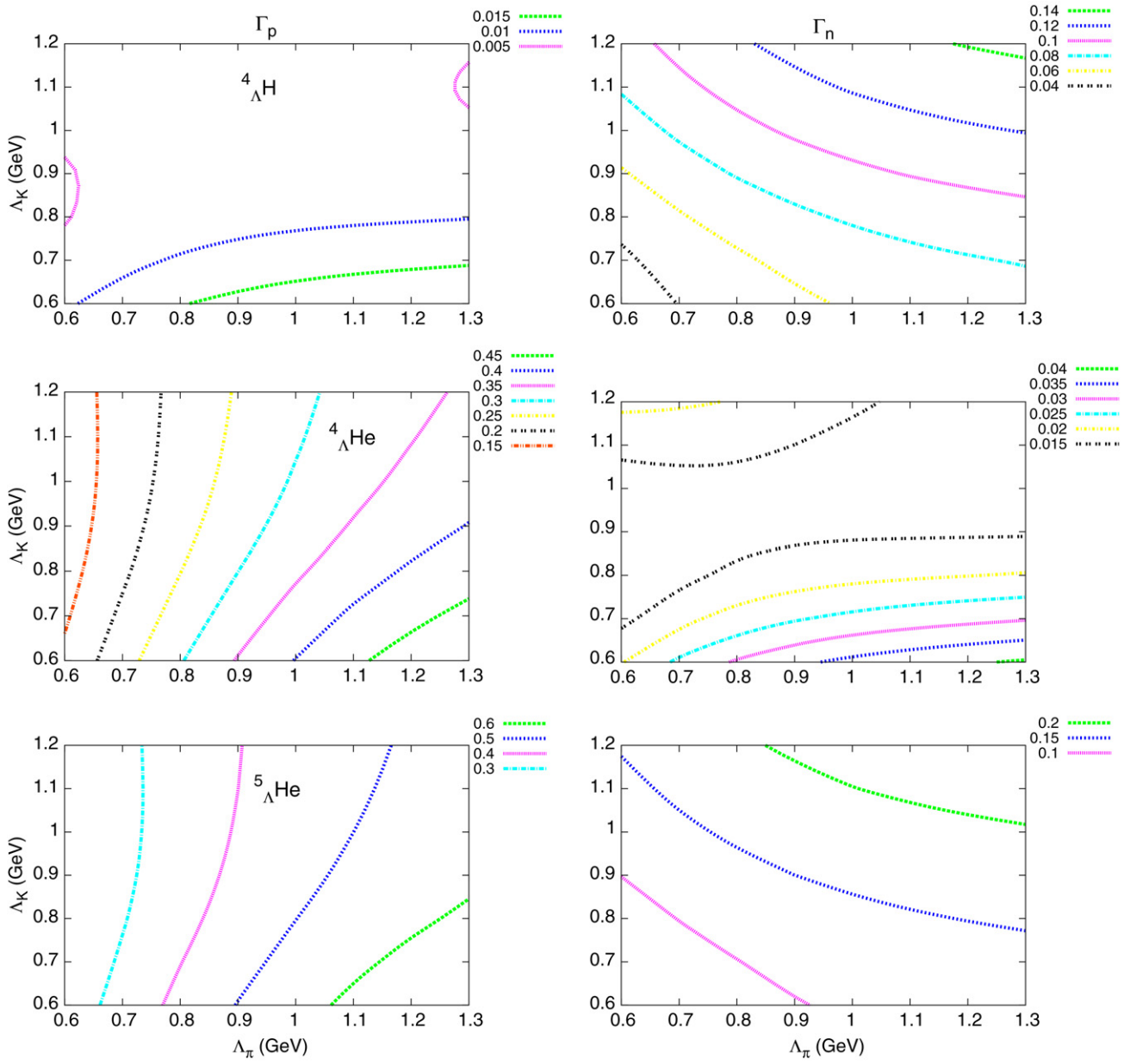

Fig. 1. Decay rates Γ_p and Γ_n of ${}^{4}_{\Lambda}$H, ${}^{4}_{\Lambda}$He and ${}^{5}_{\Lambda}$He, for fixed values of the size parameters, $b({}^{4}_{\Lambda}\mathrm{H}) = b({}^{4}_{\Lambda}\mathrm{He}) = 1.65$ fm and $b({}^{5}_{\Lambda}\mathrm{He}) = 1.358$ fm [14], as a function of pion and kaon cutoff parameters Λ_π and Λ_K.

Thus, the number of nN pairs measured in coincidence can be expressed as

$$\hat{\mathrm{N}}^{\mathrm{exp}}_{nN} = \sum_{i=1}^{k} \widetilde{\Delta \mathrm{N}}^{\mathrm{exp}}_{nN}(\cos\theta_i) = \sum_{i=1}^{l} \widehat{\Delta \mathrm{N}}^{\mathrm{exp}}_{nN}(E_i), \tag{31}$$

where the angular bins with $\cos\theta_i > -0.5$ are excluded from the first summation. The $\widetilde{\Delta \mathrm{N}}^{\mathrm{exp}}_{nN}(\cos\theta_i)$ and $\widehat{\Delta \mathrm{N}}^{\mathrm{exp}}_{nN}(E_i)$ data should be compared, respectively, with

$$\widetilde{\Delta \mathrm{N}}_{nN}(\cos\theta) = \hat{\mathrm{N}}^{\mathrm{exp}}_{nN}\, \Delta\cos\theta_{nN}\, \frac{\tilde{S}_{nN}(\cos\theta)}{\hat{\Gamma}_N}, \tag{32}$$

and

$$\widehat{\Delta \mathrm{N}}_{nN}(E) = \hat{\mathrm{N}}^{\mathrm{exp}}_{nN}\, \Delta E_{nN}\, \frac{\hat{S}_{nN}(E)}{\hat{\Gamma}_N}. \tag{33}$$

Here, from Ref. [34] $\hat{\mathrm{N}}^{\mathrm{exp}}_{np} = 4821$, $\hat{\mathrm{N}}^{\mathrm{exp}}_{nn} = 2075$, $\Delta\cos\theta_{nN} = 0.04$ and $\Delta E_{nN} = 10$ MeV, while $\hat{\Gamma}_p = 0.1709$ and $\hat{\Gamma}_n = 0.0113$. These results (Theory A) are compared with the E788 data in Figs. 3 and 4. For completeness, in the same figures are also shown the results for $\tilde{S}_{nN}(\cos\theta) \to S_{nN}(\cos\theta)$, $\hat{S}_{nN}(E) \to S_{nN}(E)$ and $\hat{\Gamma}_N \to \Gamma_N$, *i.e.*, when no energy and angular cuts are considered in the theoretical evaluation, and $\Gamma_p = 0.1793$ and $\Gamma_n = 0.0122$ (Theory B).

We conclude that the overall agreement between the measurements of Parker et al. [6] and the present calculations is quite satisfactory, although we are not considering contributions coming from the two-body induced decay, $\Lambda NN \to nNN$, nor from the rescattering of the nucleons produced in the one-body induced decay, $\Lambda N \to nN$. However, before ending the discussion we would like to point out that:

1. As expected, the theoretical spectrum $\Delta \mathrm{N}_p(E)$, shown in the upper panel of Fig. 2, is peaked around 85 MeV, corresponding to the half of the Q-value $\Delta_p = 170$ MeV. Yet, as the single kinetic energy reaches rather abruptly its maximum value $E_p^{\max} = 127$ MeV (see Eq. (13)), the proton spectrum shape is

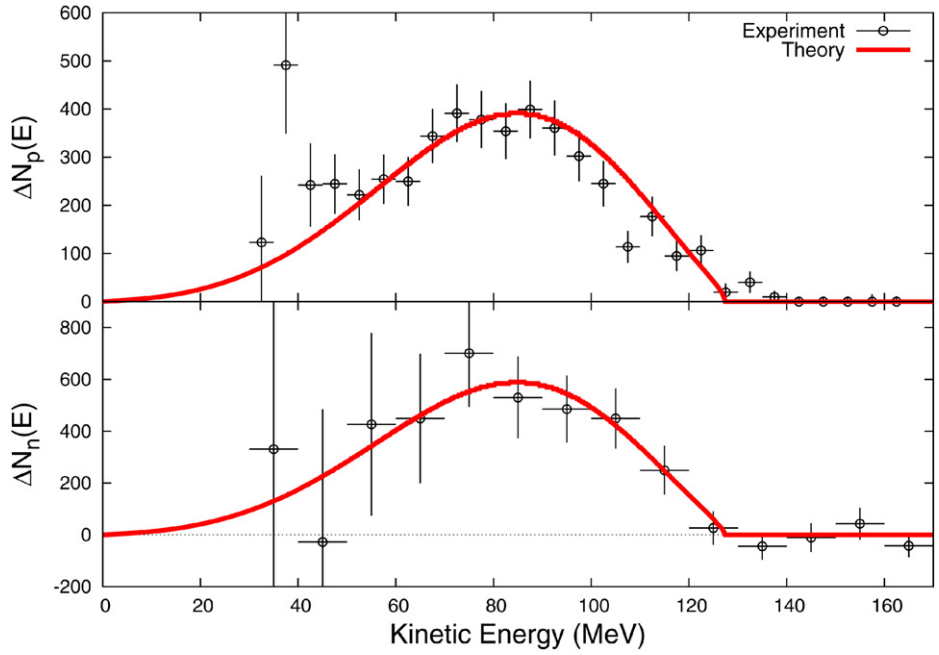

Fig. 2. Comparison between the experimental and theoretical kinetic energy spectra for protons (upper panel) and neutrons (lower panel). The data are acceptance corrected [34], and the calculated results are obtained from Eqs. (29) and (30).

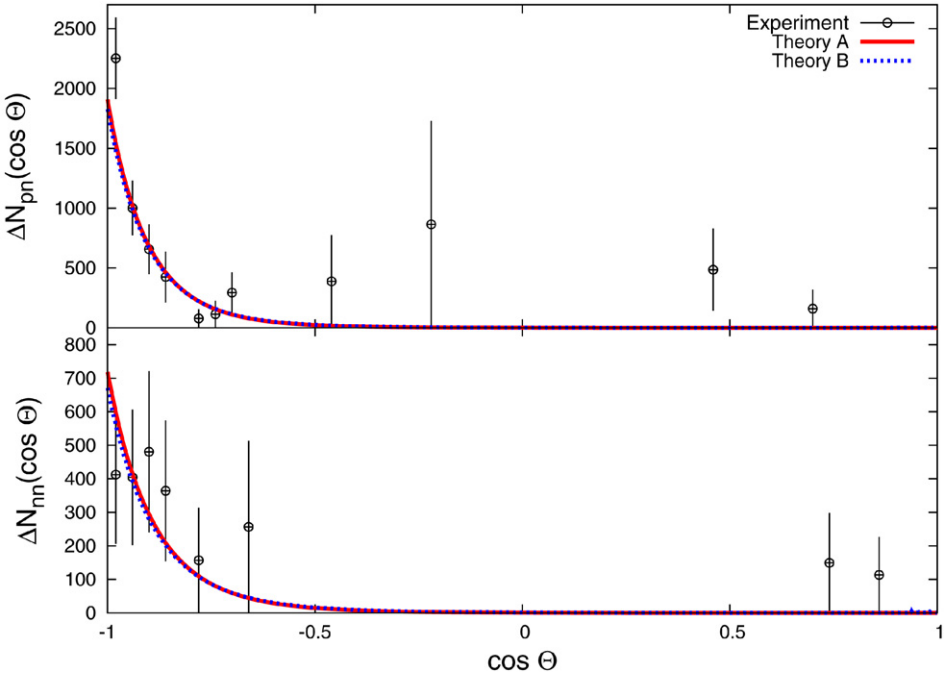

Fig. 3. Comparison between experimental opening angle correlations for proton–neutron (upper panel) and neutron–neutron (lower panel) pairs. The data $\widetilde{\Delta N}^{\rm exp}_{nN}(\cos\theta_i)$ are acceptance corrected and do not contain events with $E_N < 30$ MeV [34]. The theoretical results are obtained from Eq. (32), with $\hat{N}^{\rm exp}_{nN}$ only containing events with $\cos\theta_{nN} < -0.5$. Two cases are presented: (1) Theory A, where both the angular and the single kinetic energy cuts are taken into account, and (2) Theory B, where the cuts are not considered in the calculations.

not exactly that of a symmetric bell. Something quite analogous happens in the case of neutrons, as can be seen in the lower panel of Fig. 2. The experimental data seem to behave in the same way. To some extent, this behavior of $\Delta N_p(E)$ and $\Delta N_n(E)$ is akin to the behavior of the $\Delta N_{nN}(E)$, which suddenly collapse at the Q-values.

2. There are no data at really low energies for the proton case which would allow to exclude the FSI effects for sure, and the neutron data for low energies are afflicted by large error bars. However, there is no need to invoke these effects, nor those of two-nucleon induced NMWD, to explain the data, as occurs in the proton spectrum of ${}^{5}_{\Lambda}$He [5]. This hints at a new puzzle in the NMWD, but it is difficult to discern whether it is of experimental or theoretical nature.
3. The calculated spectra $\widetilde{\Delta N}_{np}(\cos\theta)$ shown in the upper panel of Fig. 3, are strongly peaked near $\theta = 180°$, which agrees with data fairly well. However, while it is found experimentally that 28% of events occur at opening angles less than 120°, theoretically we get that only $\lesssim 2\%$ of events appear in this angular region. We find no explanation for this discrepancy. Neverthe-

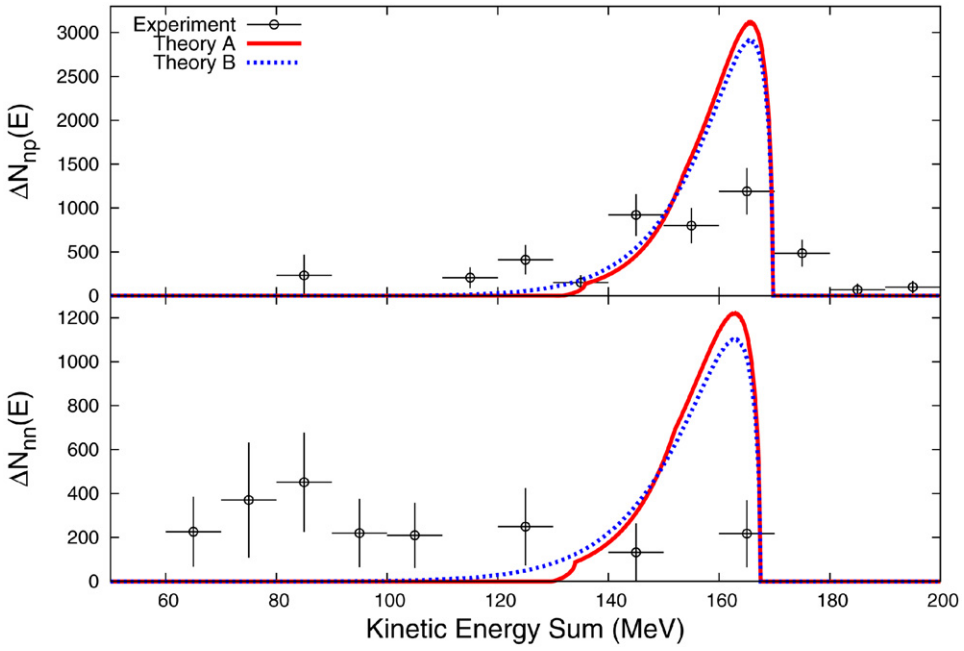

Fig. 4. Comparison between experimental kinetic energy sum spectra for proton–neutron (upper panel) and neutron–neutron (lower panel) pairs. The data $\widehat{\Delta N}^{\rm exp}_{nN}(E_i)$ are acceptance corrected and only contain events with $E_N > 30$ MeV and $\cos\theta_{nN} < -0.5$ [34]. The theoretical results are obtained from Eq. (33), and two cases are shown: (1) Theory A, where both cuts are taken into account, and (2) Theory B, where the cuts are not considered in the calculations.

less, the fact that not all events are concentrated at $\theta = 180°$, is not necessarily indicative of the contributions coming from the FSI or the $\Lambda NN \to nNN$ decay, as suggested in Ref. [6].

4. The calculated angular correlation $\widetilde{\Delta N}_{nn}(\cos\theta)$, shown in the lower panel of Fig. 3, is quite similar to that of the *pn* pair; that is, its back-to-back peak is very pronounced. This behavior is not exhibited by the experimental distribution. In addition, while 11% of events are found experimentally for $\cos\theta \geqslant -0.5$, in the calculation only $\lesssim 3\%$ of them appear at these angles. We feel however that, because of the poor statistics and large experimental errors, one should not attribute major importance to such disagreements.
5. Both calculated kinetic energy sum distributions $\widehat{\Delta N}_{nN}(E)$, shown in Fig. 4, present a bump at ≈ 160 MeV, with a width of ≈ 30 MeV, which for protons agrees fairly well with the experiment. We would like to stress once more that the spreading in strength here is totally normal even for a purely one-nucleon induced decay. The kink at ≈ 130 MeV within the Theory A comes from the angular cut, and from this one can realize that the *nN* kinetic energy sum spectra below this energy are correlated with the angular coincidence spectra $\widetilde{\Delta N}_{nN}(\cos\theta < -0.5)$. The bump observed in the experimental $\widehat{\Delta N}_{nn}(E)$ spectrum at ≈ 90 MeV is not reproduced by the theory, which may be indicative of *nn* coincidences originated from sources other than Λn decays, as already suggested in Ref. [6]. Another source for the difference between our model calculation and the data may be traced to *np* and *nn* final state interactions. Whereas in the former the intensity of this interaction is reduced owing to the Coulomb repulsion felt by the proton, in the latter the two neutrons may interact strongly and thus shift the peak to lower kinetic energy sum.

In summary, to comprehend the recent measurements in ${}^{4}_{\Lambda}$He, we have outlined for the one-nucleon induced NMWD spectra a simple theoretical framework based on the IPSM. Once normalized to the transition rate, all the spectra are tailored basically by the kinematics of the corresponding phase space, depending very weakly on the dynamics governing the $\Lambda N \to nN$ transition proper. As a matter of fact, although not shown here, the normalized spectra calculated with PSVE model are, for all practical purposes, identical to those using the SPKE model, which we have amply discussed. In spite of the simplicity of the approach, a good agreement with data is obtained. This might indicate that, neither the FSI, nor the two-nucleon induced decay processes play a significant role in the *s*-shell, at least not for ${}^{4}_{\Lambda}$He. As a byproduct we have found that the $\pi + K$ exchange potential with soft cutoffs (SPKE) is capable of accounting for the experimental values related to Γ_p and Γ_n in all three ${}^{4}_{\Lambda}$H, ${}^{4}_{\Lambda}$He, and ${}^{5}_{\Lambda}$He hypernuclei. This potential is not very different from the PKE model used by Sasaki et al. [28].

Acknowledgements

This work was partly supported by the Brazilian agencies FAPESP and CNPq, and by the Argentinian agency CONICET under contract PIP 6159. M.S.H. is the 2007/2008 Martin Gutzwiller Fellow at the Max-Planck-Institute for the Physics of Complex Systems-Dresden. We would like to thank G. Garbarino for very helpful discussions.

References

[1] P.B. Jones, Phys. Rev. Lett. 86 (2001) 1384;
P.B. Jones, Phys. Rev. D 64 (2001) 084003.
[2] J. Schaffner-Bielich, Nucl. Phys. A 804 (2008) 309.
[3] J.H. Kim, et al., Phys. Rev. C 68 (2003) 065201.
[4] S. Okada, et al., Phys. Lett. B 597 (2004) 249.
[5] M. Agnello, et al., Nucl. Phys. A 804 (2008) 151.
[6] J.D. Parker, et al., Phys. Rev. C 76 (2007) 035501.
[7] S. Okada, et al., Nucl. Phys. A 752 (2005) 169c.
[8] H. Outa, et al., Nucl. Phys. A 754 (2005) 157c.
[9] B.H. Kang, et al., Phys. Rev. Lett. 96 (2006) 062301.
[10] M.J. Kim, et al., Phys. Lett. B 641 (2006) 28.
[11] H. Bhang, et al., Eur. Phys. J. A 33 (2007) 259.
[12] A. Parreño, A. Ramos, C. Bennhold, Phys. Rev. C 56 (1997) 339.
[13] A. Parreño, A. Ramos, Phys. Rev. C 65 (2002) 015204.
[14] K. Itonaga, T. Ueda, T. Motoba, Phys. Rev. C 65 (2002) 034617.

[15] C. Barbero, D. Horvat, F. Krmpotić, T.T.S. Kuo, Z. Narančić, D. Tadić, Phys. Rev. C 66 (2002) 055209.
[16] F. Krmpotić, D. Tadić, Braz. J. Phys. 33 (2003) 187.
[17] C. Barbero, C. De Conti, A.P. Galeão, F. Krmpotić, Nucl. Phys. A 726 (2003) 267.
[18] J.F. Dubach, G.B. Feldman, B.R. Holstein, L. de la Torre, Ann. Phys. (N.Y.) 249 (1996) 146.
[19] A.H. Wapstra, N.B. Gove, Nucl. Data Tables 9 (1971) 265.
[20] N.N. Kolesnikov, S.A. Kalachev, Phys. At. Nucl. 69 (2006) 2020.
[21] C. Barbero, A.P. Galeão, F. Krmpotić, Phys. Rev. C 72 (2005) 035210.
[22] C. Barbero, A.P. Galeão, F. Krmpotić, Phys. Rev. C 76 (2007) 0543213.
[23] F. Krmpotić, A.P. Galeão, C. Barbero, in: Proceedings of the 23th International Nuclear Physics Conference, Tokyo, Japan, 3–8 June 2007, Nucl. Phys. A 805 (2008) 194.
[24] C. Barbero, A.P. Galeão, M. Hussein, F. Krmpotić, Phys. Rev. C 78 (2008) 044312; C. Barbero, A.P. Galeão, M. Hussein, F. Krmpotić, Phys. Rev. C 78 (2008) 059901, Erratum.
[25] H. Outa, et al., Nucl. Phys. A 639 (1998) 251c.
[26] T. Inoue, M. Oka, T. Motoba, K. Itonaga, Nucl. Phys. A 633 (1998) 312.
[27] J.H. Jun, Phys. Rev. C 63 (2001) 044012.
[28] K. Sasaki, T. Inoue, M. Oka, Nucl. Phys. A 707 (2002) 477.
[29] K. Sasaki, M. Izaki, K. Itonaga, M. Oka, Phys. Rev. C 71 (2005) 035502.
[30] W.M. Alberico, G. Garbarino, A. Parreño, A. Ramos, Phys. Rev. Lett. 94 (2005) 082501.
[31] C. Chumillas, G. Garbarino, A. Parreño, A. Ramos, Phys. Lett. B 657 (2007) 180.
[32] K. Itonaga, T. Motoba, T. Ueda, Th.A. Rijken, Phys. Rev. C 77 (2008) 044605.
[33] C. Bennhold, A. Ramos, Phys. Rev. C 45 (1992) 3017.
[34] J.D. Parker, private communication.
[35] W.T. Winter, S.J. Freedman, K.E. Rehm, J.P. Schiffer, Phys. Rev. C 73 (2006) 025503.